Stem Cell Research (2014) 13, 284–299

Available online at www.sciencedirect.com

ScienceDirect

www.elsevier.com/locate/scr

Primary cilium-associated genes mediate bone marrow stromal cell response to hypoxia

James A.L. Brown[a,b,1], Tapesh Santra[c], Peter Owens[d], Aline M. Morrison[b], Frank Barry[a,b,*]

[a] Systems Biology Ireland, Regenerative Medicine Institute (REMEDI), National University of Ireland, Galway, Ireland
[b] Regenerative Medicine Institute (REMEDI), National University of Ireland, Galway, Ireland
[c] Systems Biology Ireland, Conway Institute, University College Dublin (UCD), Dublin, Ireland
[d] Centre for Microscopy and Imaging, Anatomy Department, National University of Ireland, Galway, Ireland

Received 12 March 2014; received in revised form 27 June 2014; accepted 28 June 2014
Available online 8 July 2014

Abstract Currently there is intense interest in using mesenchymal stem cells (MSC) for therapeutic interventions in many diseases and conditions. To accelerate the therapeutic use of stem cells we must understand how they sense their environment. Primary cilia are an extracellular sensory organelle present on most growth arrested cells that transduce information about the cellular environment into cells, triggering signaling cascades that have profound effects on development, cell cycle, proliferation, differentiation and migration.

Migrating cells likely encounter differing oxygen tensions, therefore we investigated the effect of oxygen tension on cilia. Using bone marrow stromal cells (BMSCs, also known as bone marrow-derived mesenchymal stem cells) we found that oxygen tension significantly affected the length of cilia in primary BMSCs. Chronic exposure to hypoxia specifically down-regulated genes involved in hedgehog signaling and re-localized the Smo and Gli2 proteins to cilia. Investigating the effects of chemotactic migration on cilia, we observed significantly longer cilia in migrating cells which was again, strongly influenced by oxygen tension. Finally, using computational modeling we identified links between migration and ciliation signaling pathways, characterizing the novel role of HSP90 and PI3K signaling in regulating BMSC cilia length.

These findings enhance our current understanding of BMSC adaptions to hypoxia and advance our knowledge of BMSC biology and cilia regulation.

Abbreviations: BMSC, bone marrow-derived mesenchymal stem cell; MSC, mesenchymal stem cell; SFM, serum free media; Hypoxia, 5% O_2; Normoxia, 20% O_2; PBS, phosphate buffered saline; MIP, maximum intensity projections; PI, propidium iodide; MTOC, microtubule organizing center; PCM, pericentriolar material; PI3K, phosphatidylinositide 3-kinase.

* Corresponding author.
E-mail addresses: james.brown@nuigalway.ie (J.A.L. Brown), tapesh.santra@gmail.com (T. Santra), peter.owens@nuigalway.ie (P. Owens), aline.morrison@nuigalway.ie (A.M. Morrison), frank.barry@nuigalway.ie (F. Barry).
[1] Currently: Discipline of Surgery, School of Medicine, National University of Ireland, Galway, Ireland.

http://dx.doi.org/10.1016/j.scr.2014.06.006
1873-5061/

Introduction

Primary cilia (non-motile) are cellular extensions extending from most growth arrested mammalian cells and are responsible for coordinating responses to extracellular conditions (Basten and Giles, 2013; Christensen et al., 2008; Quarmby and Parker, 2005; Satir et al., 2010). Primary cilia sense the extra-cellular environment by chemosensation and mechanotransduction, transducing this information through signaling cascades, allowing cells to respond to environmental stimuli (Avasthi and Marshall, 2012; Davenport and Yoder, 2005; Han et al., 2008; Malone et al., 2007; Oh and Katsanis, 2012). The primary cilium is comprised of two main parts: 1) a basal body, consisting of modified centrioles and 2) a ciliary axoneme, comprised of a ring of 9 microtubule doublets bound by the cell membrane. As sensory organs primary cilia [9(+0)] lack the central structural microtubule doublet (+2) and dynein arms required for motile cilia [9(+2)] (Basten and Giles, 2013; Takeda and Narita, 2012). Importantly, defects in primary cilia have been found to be the causative agent behind many human diseases or developmental defects (Nigg and Raff, 2009; Oh and Katsanis, 2012; Pan et al., 2005; Schmidt et al., 2012; van Reeuwijk et al., 2011; Weatherbee et al., 2009; Zalli et al., 2012).

Centrosomes, consisting of a pair of mother and daughter centrioles, are the major microtubule organizing center (MTOC) for the cell and are crucial for correct separation of replicated DNA (Avasthi and Marshall, 2012; Davenport and Yoder, 2005; Han et al., 2008; Malone et al., 2007; Mardin and Schiebel, 2012; Oh and Katsanis, 2012), migration and orientation (Basten and Giles, 2013; Gotlieb et al., 1983; Li and Gundersen, 2008; Petrie et al., 2009; Schneider et al., 2010; Takeda and Narita, 2012). Primary cilia form in growth arrested cells (G_0/G_1 cell cycle phase) following centrosome re-localization to the cell membrane. There the centrosome matures, accumulating pericentriolar (PCM) material and acquiring distal and subdistal appendages, forming a basal body. Basal bodies anchor the cilia, which extend from the mother centriole (Avasthi and Marshall, 2012; Bornens, 2012; Nigg and Raff, 2009; Nigg and Stearns, 2011; Oh and Katsanis, 2012; Pan et al., 2005; Reiter et al., 2012; Satir et al., 2010; Schmidt et al., 2012; van Reeuwijk et al., 2011; Weatherbee et al., 2009; Zalli et al., 2012). Processes controlling centrosome duplication and basal body formation are cell cycle dependent and tightly regulated, as centrosome overduplication can lead to genomic instability (Azimzadeh and Marshall, 2010; Bourke et al., 2010; Brown et al., 2010; Ganem et al., 2009).

Bone marrow stromal cell populations (BMSCs, also known as bone marrow-derived mesenchymal stem cells) are known to contain a subset of stem cells that are infrequently replicating, multipotent cells commonly thought to reside in hypoxic niches in the bone marrow, important for maintaining their undifferentiated state (Basciano et al., 2011). This suggests that oxygen tension plays an important role in stem cell regulation and indeed oxygen tension was recently found to affect BMSC differentiation (Basciano et al., 2011; Berniakovich and Giorgio, 2013). Previously, stem cell cilia have been implicated in differentiation and lineage commitment (Han et al., 2008; Hoey et al., 2012; Tummala et al., 2010). Currently, a strong need to better understand how stem cells sense their environment exists, yet very little is known about the primary cilia of BMSCs. Serum starving stem cells will induce ciliation (Bornens, 2012; Seeley and Nachury, 2010) and it has been previously reported that cultured BMSCs exhibit primary cilia (Hoey et al., 2012). Recent results demonstrate that the effects of oxygen tension on cilia induction or length are variable, affecting cilia in non-serum-starved chondrocytes (Wann et al., 2013) but not serum-starved immortalized human retinal pigmented epithelial (RPE-1) cells (Troilo et al., 2014). Previously, acute exposure to 2% hypoxia was shown to reduce ciliation (Proulx-Bonneau and Annabi, 2011). Yet, the effects of chronic hypoxic exposure on primary cilia are unknown. Additionally, the consequences of chemotactic migration on primary cilia length remain undetermined.

We characterized primary BMSCs by investigating the effects of oxygen tension and chemotactic migration on primary cilia frequency and length. We further examined cilia specific gene expression and protein localization to primary cilia, in response to chronic hypoxia exposure. Using computational modeling we explored the interactions between ciliation and migration pathways, predicting key proteins linking the two processes. Using inhibitors we then validated a key molecule our predictive modeling identified as linking ciliation and migration (HSP90). Exploring this further we examined the role of the associated PI3K signaling pathway.

Materials and methods

BMSC isolation and cell culture conditions

Primary BMSCs were isolated from 8 to 10 week old BALB/c mice (Jackson Laboratories) as previously described (Sugrue et al., 2012). Briefly, marrow was extracted from the femurs and tibiae, crushed, washed and plated directly onto plastic in alpha MEM (Gibco), supplemented with 10% equine serum (Hyclone, Thermo Scientific), 10% FBS (Hyclone, Thermo Scientific), and 1% penicillin/streptomycin (Invitrogen). Cells were cultured for 14–22 days to deplete the non-adherent hematopoietic cells. BMSCs were confirmed to contain a subset of stem cells by their ability to differentiate into chondrocytes, adipocytes and osteoblasts as previously described (Sugrue et al., 2013; Sullivan et al., 2012) (data not shown). >3 donor mice were used to establish the BMSC cultures. All animal work was approved by the National University of Ireland Galway Ethics Committee and were conduced in compliance with the "Principles of Laboratory Animal Care" formulated by the National Society for Medical Research and the "Guidelines for the Care and Use of Laboratory Animals" prepared by the National Academy of Science, which was published by the National Institutes of Health (ISBN 0-309-05377-3, revised 1996). All experiments were performed on BMSCs between passages 3 and 7. Cells were cultured at 37 °C in either 5% (in an O_2 controlled incubator) or 20% O_2, as indicated. BMSCs were serum-starved for indicated times to induce ciliogenesis.

Cilia stimulation and drug treatments

BMSCs were cultured in serum-free conditions, with or without indicated drugs, for 24 h prior to all assays. Drugs

were used at the following concentrations: PI3K inhibitor: 5 μM LY-294002 (Merck), HSP90aa1 inhibitor: 10 μM AUY922 (HY-10215, MedChem Express), 20 ng/ml MCP-1 (479-JE, R&D Systems), and 10 μM Y27632 (Sigma).

Flow cytometry

Propidium iodide staining was performed as previously described (Brown et al., 2010). Briefly, cells were trypsinized

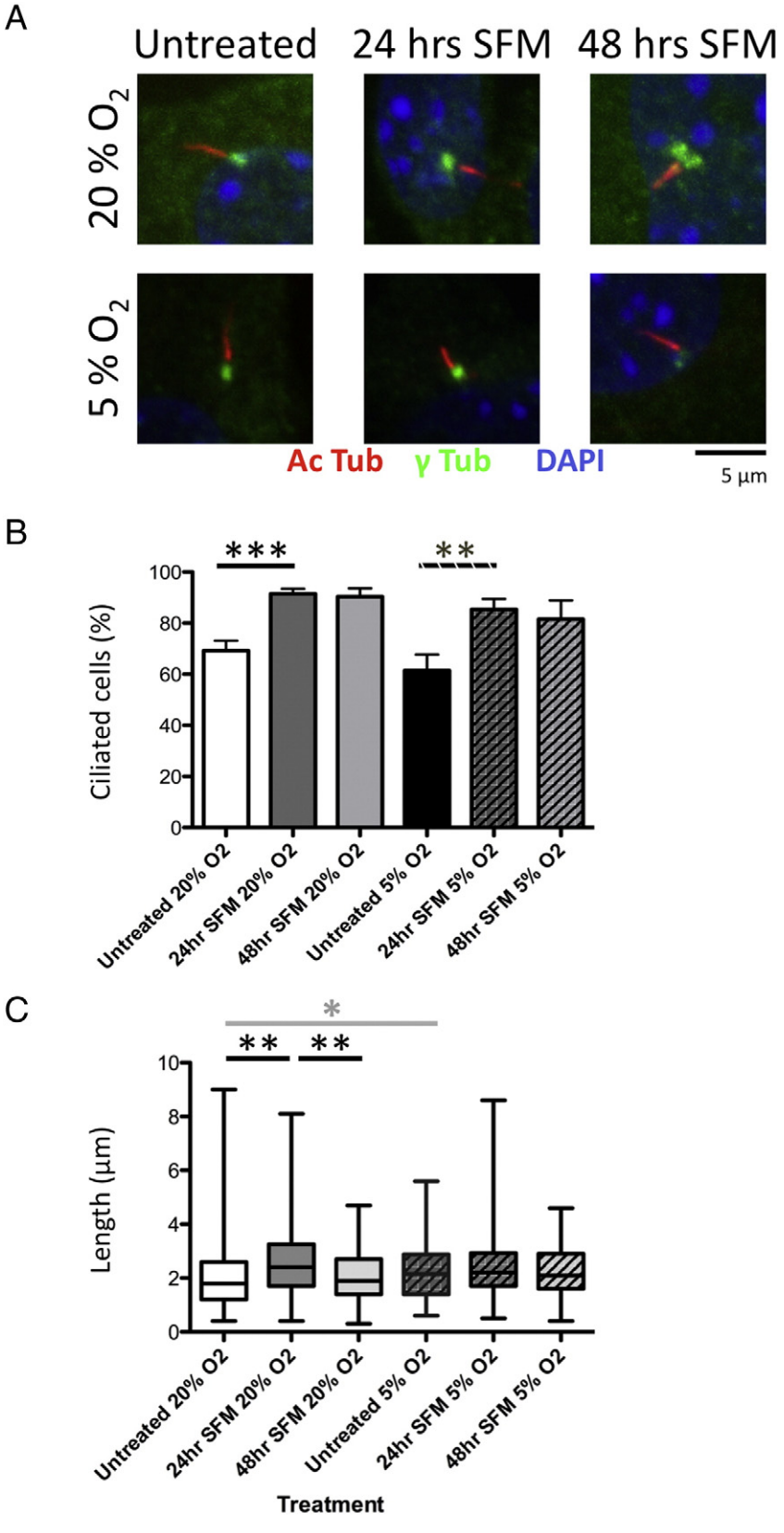

and washed in phosphate buffered saline (PBS) (Gibco, Life Technologies), fixed in ice cold 70% ethanol, washed in PBS and then stained with propidium iodide (40 mg/ml) in PBS containing RNase A (100 mg/ml) (Sigma). Following this, cells were analyzed on a FACS Canto (BD Biosciences, Erembodegem, Belgium) and the percentage of cells in G1, S, and G2/M phases of the cell cycle were analyzed using the propidium iodide staining profile.

2D chemotaxis assay system

Migration was assessed in a 2D chemotaxis system (μ-slide chemotaxis^{2D}, IBIDI) according to the manufacturer's instructions. Briefly, BMSCs were seeded onto the μ-slide and allowed to adhere for 24 h. Cells were then serum depleted for 24 h, with or without the indicated drug treatments, prior to initiation of the assay. Indicated chemo-attractants were added, as per manufacturer's instructions, for the indicated times. Cells were then fixed with 4% paraformaldehyde and permeabilized with 0.1% Triton X-100 (Sigma) prior to staining (described below).

Immunofluorescence

BMSCs were seeded onto glass slides and stained as previously described (Brown et al., 2011). Briefly, cells were fixed in 4% paraformaldehyde and permeabilized with PBS/0.1% Triton X-100. Fixed cells were then blocked in PBS/0.1% Triton X-100/1% BSA and stained with the indicated antibodies at 37 °C for 1 h. Cells were washed and incubated with the appropriate secondary antibody as indicated below. BMSC DNA was then stained using DAPI (Invitrogen) and the slides mounted using slowfade gold anti-fade reagent (Invitrogen). Immunofluorescent Z-stack images (0.1 μm steps) were captured using an Olympus IX81 Microscope fitted with an Andor Revolution Confocal system (Andor, Belfast, Northern Ireland), 60× oil immersion objective lens and an EMCCD Andor iXon^{EM+} camera. All Z stack images were processed using Andor IQ 2.3 software and all images are presented as maximum intensity projections (MIP). Acetylated α-Tubulin marked cilia were measured from MIP, from base (centrosome marked) to tip, using calibrated ImageJ software (Schneider et al., 2012).

Antibodies

Primary antibodies: F-Actin Rhodamine-conjugated phalloidin (P1951, Sigma), α-Tubulin (Clone B-5-1-2, Sigma), acetylated α-Tubulin (D20G3, Cell Signaling), γ-Tubulin (GTU-88, Sigma), Smo (E-5: sc-166685, Santa Cruz), Gli2 (H-300: sc-28674, Santa Cruz), Isotype controls: Mouse and rabbit (Thermo Fisher Scientific Inc.). Secondary antibodies: Cy3-labeled anti-rabbit antibody (Jackson ImmunoResearch Europe), FITC-labeled anti-goat IgG antibody (Santa Cruz Biotechnology), Dylight 488-labeled anti-mouse antibody (Thermo Fisher Scientific Inc.). All primary antibodies were used at 1/100 dilution and secondary antibodies at 1/200 dilution.

Mouse primary cilia RT^2 profiler PCR array

The 384 well plate mouse primary cilia RT^2 PCR assay (PAMM-127Z, QIAGEN) against 84 key cilia genes was used according to the manufacturer's instructions. Arrays were run on the Roche LightCycler 480 II Real Time PCR System with a SYBR Green qPCR Master Mix (QIAGEN). cDNA synthesis and real-time PCR were performed as per the manufacturer's instructions (QIAGEN). Quantitative RT-PCR was performed with gene expression (relative) calculated, with each replicate cycle threshold (Ct) normalized to the average Ct of four endogenous control genes (B2M, GAPDH, ACTB and GUSB). Fold change values are then presented as average fold change >2 (average $^{\Delta}$Ct). Data from multiple independent arrays (n, indicated in figure legends) was analyzed using Qiagen RT^2 profiler PCR array data analysis version 3.5 (http://pcrdataanalysis.sabiosciences.com/pcr/arrayanalysis.php).

Computational modeling

A list of proteins/genes (and approximate numbers of each) was assembled from the literature and this list then used to create a network: migration (~200), centrosomes (~350), ciliation (~200) or cell cycle (~20) [assembled, not exclusively from: (Arnaiz et al., 2009; Branzei and Foiani, 2008; Ishikawa et al., 2012; Kim et al., 2010; Seeley and Nachury, 2010; Simpson et al., 2008; van Reeuwijk et al., 2011)]. In the network proteins were identified using three steps: (1) a reconstructed proteome wide protein–protein interaction network, systematically integrating data from several databases. (2) Extraction of a small sub-network, which consists of the proteins participating in the indicated pathways and (3) a centrality analysis on the extracted sub-network, to uncover proteins that appear to be critical for information flow from one part of the sub-network to another part. Below we discuss these steps in detail.

Reconstructing proteome-wide protein–protein interaction network

To reconstruct proteome wide protein–protein interaction (PPI) network, we downloaded protein interaction data from several PPI and post-translational protein modification (PPM) databases. For PPI data we chose BIND (Bader et al., 2003), STRING (Prasad et al., 2009), BioGrid (Stark et al., 2011), and HPRD (Szklarczyk et al., 2011). For PPM data we chose PhosphoELM (Dinkel et al., 2011) and PhosphoSitePlus (Hornbeck et al., 2012) databases. As different PPI and PPM databases use different naming conventions we first mapped

Figure 1 Oxygen tension and serum starvation effect BMSC cilia. A. BMSCs grown under 20% and 5% O_2 tension had cilia induced by 24 or 48 h serum starvation. Cilia visualized by staining with acetylated α-Tubulin (red). Centrosomes visualized by staining for γ-Tubulin (green). DNA stained with DAPI (blue). Scale bar = 5 μm. B. Percentage of BMSC displaying cilia, grown under 20% (left) or 5% (right) O_2 tension, following the indicated treatments. Graph represents N = 5 (>100 cells evaluated for each separate independent experiment). C. Cilia length following indicated treatments under 20% O_2 (left) or 5% O_2 (right) tension. Graph represents N = 5 (>40 cilia evaluated for each separate independent experiment). Cilia measured from base (centrosome marked) to tip. A P-value <0.05(*) was deemed significant, $P < 0.01$(**) very significant, and a $P < 0.001$(***) highly significant. Graph displays median, +/−interquartile range and maximum and minimum measurements.

different protein IDs of all datasets into standard gene symbols by using ID mapping tools (Alibés et al., 2007). This allowed us to integrate data from many different databases permitting us to seamlessly integrate data from heterogeneous sources. Then, we removed redundant interactions from the resulting ensemble of interaction data. To increase the quality of our dataset we kept only experimentally determined interactions, discarding interactions predicted by computational means only. The interactions of the resulting dataset were then divided into two groups, protein binding and post-translational modifications. In the reconstructed PPI network, the protein binding interactions were represented by undirected edges and the PPM interactions were represented by directional edges. We then identified the sub-network of the resulting network, which is involved in ciliogenesis, migration or cell cycle.

Extracting sub-networks
Initially, we identified a list of proteins participating in the sub-network using the list of proteins utilized to create the network. We then identified the shortest paths (in the reconstructed PPI network) that connect these proteins to each other (Sniedovich, 2006). If two proteins directly interact with each other, the shortest path between them consists of only one protein interaction. But, if two proteins do not directly interact with other, the shortest path between them consists of a chain of protein interactions, which originates in one of the two proteins and terminates in another. In such cases, the path (or chain of interactions) may contain proteins that do not directly participate in any of the sub-networks. We call these proteins "connectors". The extracted sub-network consists of the proteins that directly participate in the above pathways, the "connector" proteins and all interactions among these proteins.

Identifying the critical nodes in the extracted sub-network
To identify the critical proteins in the sub-network, we calculated between-ness and Eigen-vector centrality (Opsahl et al., 2010) measures for each of its component proteins. The between-ness centrality quantifies the number of times a network node (in this case a protein) acts as a bridge along the shortest path between two other nodes (proteins) (Opsahl et al., 2010). Proteins with highest between-ness centrality measures acted as junctions, through which majority of the information flowed from one part of the network to another. Conversely, Eigenvector centrality quantifies the influence of a protein in the network. Proteins with the highest eigenvector centralities are those connected to the most well connected proteins in the network, i.e. proteins regulating large hubs. The proteins with the highest between-ness and Eigenvector centralities were considered to be critical for the integrative functioning of the sub-networks.

Statistical analyses

To avoid any bias, primary cilia counts and lengths were recorded from multiple fields from the indicated number of independent cell culture preparations. Data analyses were performed using Prism 5 software (GraphPad Software, Inc., La Jolla, CA, USA). Statistical significance was calculated with a One-way ANOVA using a Kruskal–Wallis test with a posthoc Dunn's or Tukey test to evaluate the statistical significance between groups, unless otherwise indicated. A P-value <0.05(*) was deemed significant, $P < 0.01$(**) very significant and $P < 0.001$(***) highly significant, as stated in the figure legends. Values of the counts of cilia incidence or measurements of cilia length represent at least 3 separate discrete experiments with >30 measurements/counts made for each separate independent experiment (n and minimum number measurements for each separate experiment indicated in figure legends). Graphs 1C, 4B, 6D and 7B display median (+/−interquartile range) and maximum and minimum measurements, as indicated in figure legends. All other graphs display mean (+/−SEM). Experiments for Figs. 6C–D and & 7A–B were conducted in parallel and share a common set of untreated controls.

Results

Serum starvation induces BMSC primary cilia formation

Primary BMSCs are cultured in vitro under both normoxic and hypoxic conditions, yet the long-term effects, on primary cilia, of culturing BMSCs under different oxygen (O_2) tensions have not been explored. Previous work has investigated effects on primary cilia using cells grown under normoxic conditions and subjected to acute (up to 72 h) exposure to hypoxic conditions. Additionally, we sought to confirm if serum starvation of BMSCs would induce cell cycle arrest and ciliation, as previously reported (McMurray et al., 2013; Satir and Christensen, 2007; Zhu et al., 2009a). To determine the basal level of ciliation primary BMSCs were stained for the cilia marker, acetylated α-Tubulin and the centrosome marker γ-tubulin (Figs. 1A, S1A–B). In addition, we observed that BMSC cilia could be readily visualized by α-Tubulin staining (Fig. S1C). Basal ciliation levels were assessed in BMSCs grown under normoxic (20% O_2) or hypoxic (5% O_2) oxygen tension (Figs. 1A and B: 20% O_2—white bar and 5% O_2—black bar). We found that 60–70% of BMSCs are ciliated under normal growth conditions, regardless of oxygen tension. We then examined if serum starvation induced ciliation in BMSCs grown under either normoxic or hypoxic conditions (Figs. 1A–B, S1A–B). Treatment with 24 h of SFM under normoxic conditions induced a highly significant [$P < 0.001$(***)] 32% induction in ciliation, compared to untreated cells [91.5% (±4.8%) compared to 69% (±12.5%)]. Under hypoxic conditions 24 h of SFM treatment induced a very significant [$P < 0.01$(**)] 39% induction in ciliation [85.5% (±9.1%) compared to 61.5% (±19.7%)] (Fig. 1B: 20% O_2: single colored bars and 5% O_2: hatched bars). Statistical analysis revealed no further significant results. We confirmed that serum starvation arrested cell growth in our system (Fig. S2A), as indicated by a significant [$P < 0.05$(*)] ~80% reduction of cells in the S phase of the cell cycle, regardless of oxygen tension [untreated ~5%; 24 h SFM treatment ~0.9%] (Fig. S2B). The number of cells observed in G_0/G_1 correlated well with the level of cilia positive cells previously observed (Fig. 1B). Following serum starvation a small number of cells were observed in G_2 (<10% cells), however manual analysis indicated that these were binucleate cells (Fig. S2C). The number of binucleate cells observed remained relatively constant, regardless of oxygen

tension or treatment and were excluded from all analyses performed.

Oxygen tension affects primary cilia length

The physical size of a cilium will affect its ability to accurately sense a chemical gradient (Berg and Purcell, 1977; Bialek and Setayeshgar, 2005; Skoge et al., 2010; Wicher, 2012). However, the effects of long-term exposure to differing oxygen tensions, alone or in combination with serum starvation, on primary cilia length have not been investigated in BMSCs. Investigating BMSCs cultured under normoxic conditions we found that 24 h SFM treatment induced a very significant [$P < 0.01$(**)] 33% increase in cilia length from 1.8 to 2.4 μm (median values) (variation 0.4–9.0 and 0.4–8.1 μm, respectively) (Fig. 1C—single colored bars). Furthermore, under normoxic conditions we observed a significant [$P < 0.01$(**)] 21% reduction in cilia length in BMSCs exposed to 48 h of SFM treatment (median value: 1.9 μm: variation 0.4–4.7 μm) compared to 24 h (median value: 2.4 μm: variation 0.4–8.1 μm). However, the cause of this reduction was not explored further. Under hypoxic conditions, no significant effects on cilia length were observed following SFM-mediated cilia induction (median lengths of 2.15, 2.2 and 2.1 μm: variation 0.6–5.6, 0.5–8.6 and 0.4–4.6 μm, respectively) (Fig. 1C—hatched bars). However, comparing cilia length across oxygen tensions, we found that there was a significant [$P < 0.05$(*)] 19% increase in cilia length in untreated BMSCs grown under hypoxic oxygen tension (median value 2.15 μm: variation 0.6–5.6 μm), compared to normoxia (median value 1.8 μm: variation 0.4–9.0 μm).

BMSC populations contain cells with split and amplified centrosomes

As cilia biogenesis is intimately linked to centrosomes, we investigated the effects of 20% or 5% oxygen tension, alone or in combination with serum starvation, on centrosomes. We found that under all conditions assayed BMSCs had low levels of centrosome amplification (≥3 centrosomes, Figs. 2A–B and S3). Furthermore, we did not observe any significant changes in centrosome amplification upon SFM-induced cilia induction. Interestingly, only BMSCs grown under 20% O_2 tension had a statistically significant increase [$P < 0.05$(*)] in the number of twin γ-tubulin foci observed following SFM treatment (42% rising to 62%), which is indicative of centrosome splitting (Fig. 2C). Analysis of all other treatments was performed, however no statistical significance was found (Figs. S3A–B).

Hypoxia down-regulates genes involved in Hh signaling

To further understand how the long-term growth of BMSCs in hypoxia induced changes in the cilia, we examined the expression levels of a panel of cilia related genes using a PCR array (Fig. 3A). We found that two genes were >2 fold up-regulated (Fos and Vangl2) (Fig. 3A, red tiles) and 11 genes were >2 fold down-regulated (Fig. 3A, gray and light green tiles). The list of misregulated genes found is shown in Table 1. Mapping the down-regulated genes using STRING (Szklarczyk et al., 2011), we found that several identified genes were members of the Hedgehog (Hh) signaling pathway (Fig. 3B).

To further explore this we investigated additional consequences of the observed mRNA down-regulation, on selected proteins in the Hh signaling pathway, such as re-localization. In addition to the down-regulation of Smo mRNA observed under hypoxic conditions, Smo proteins re-localized to the base of primary cilia (Figs. 3C—white arrowhead, S4A). Furthermore, hypoxic down-regulation of Smo and Fzd-1 mRNA resulted in re-localization of their target, transcription factor Gli2, into the primary cilia (Figs. 3D—white arrowhead, S4B).

MCP-1 induces significant BMSC migration

Several of the genes down-regulated under hypoxic conditions are implicated in mediating cell migration or microtubule re-organization (Smo, Fzd-1, Ihh, Rock2, Bbs1, Cdk5rap2 and Pkd1) (Döppler et al., 2013; Fong et al., 2009; Ishizuka et al., 2011; Kulaga et al., 2004; Laeremans et al., 2010; Lin et al., 2012; Shinozaki et al., 2008) or target the Gli transcription factors, resulting in inhibition of migration (Chen et al., 2014). We therefore examined the effects of oxygen tension on chemotactic-mediated migration and primary cilia orientation in BMSCs. To stimulate chemotactic migration we used fetal calf serum (FCS) as a non-specific chemoattractant and Monocyte Chemoattractant Protein 1 (MCP-1), a known chemoattractant. Although both FCS and MCP-1 induced migration regardless of oxygen tension, we found that MCP-1 induced a very significant [$P < 0.01$(**)] ~8 fold increase in migration of BMSCs under normoxic conditions (Fig. 4A—single colored bars). In addition, under hypoxic conditions MCP-1 induced a significant [$P < 0.05$(*)] ~4 fold increase in migration of BMSCs (Fig. 4A—hatched bars). Although there was a marked reduction in the efficiency of both FCS and MCP-1 stimulated migration in BMSCs grown under hypoxic conditions, compared to normoxic conditions, the difference did not reach statistical significance.

Chemoattraction-mediated migration significantly affects primary cilia length

To assess if migration affected the structure of BMSC primary cilia we analyzed the length of the cilia on chemotactically-stimulated, migrating BMSCs. Investigating cilia length in a single oxygen tension we found that under normoxic conditions FCS-induced migration resulted in a highly significant [$P < 0.001$(***)] 34% increase in cilia length, compared to MCP-1 (median values 2.25 compared to 1.68 μm; variations 1.0–4.8 and 0.63–4.96 μm, respectively) (Fig. 4B—single colored bars). Under hypoxic conditions FCS-mediated migration induced a highly significant [$P < 0.001$(***)] 26% increase in cilia length, compared to SFM alone (median values: 2.53 compared to 2.01 μm; variations 0.75–7.0 and 0.7–4.44 μm, respectively) (Fig. 4B—hatched bars). Comparing the effects of MCP-1 mediated migration across oxygen tensions we found that under hypoxic conditions BMSC cilia had a significant [$P < 0.001$(***)] 42% increase in length (median value: 2.39 μm; variation 1.04–6.17 μm), compared to those observed under normoxic conditions (median value: 1.68 μm; variation 0.63–4.96 μm). Similarly, compared to cilia observed on normoxic SFM treated BMSCs (median value: 1.82 μm; variation 0.75–4.52 μm) we found that significant increases in cilia length on BMSCs grown under hypoxic conditions and chemoattracted with either FCS,

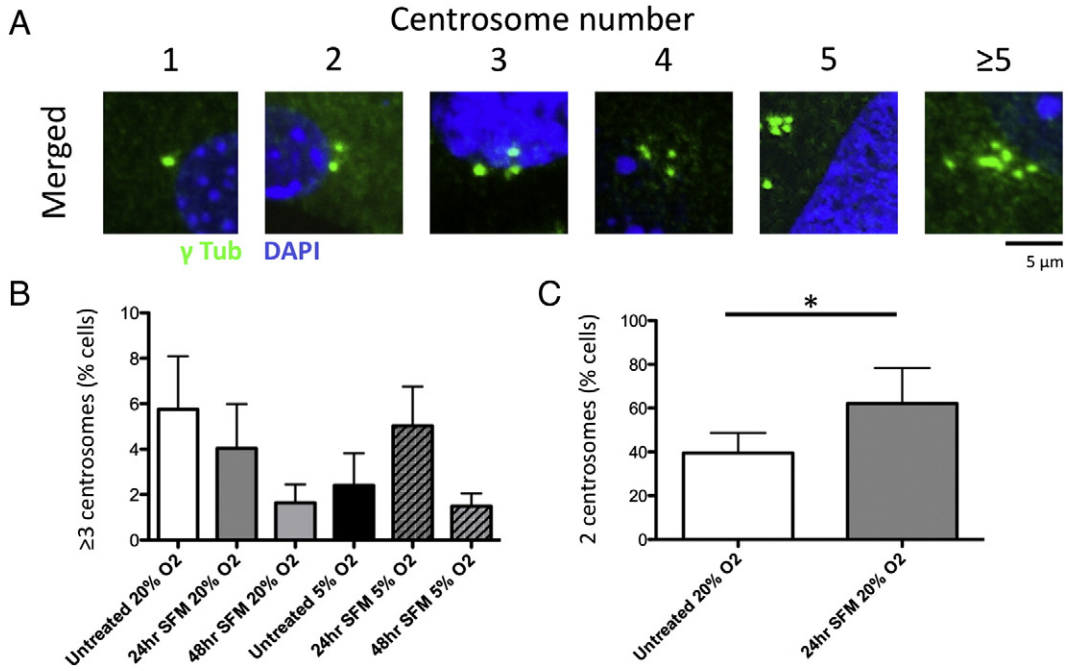

Figure 2 Centrosome amplification in primary BMSCs. A. Representative images of centrosome counts. Centrosomes visualized by staining for γ-Tubulin (green). DNA stained with DAPI (blue). Scale bar = 5 μm. B. Centrosome amplification counts in BMSCs grown under 20% (left) or 5% (right) O_2 tension, following the indicated treatments. C. Count of cells displaying 2 distinct centrosomes following the indicated treatments under 20% O_2. Graphs represent N = 3 (>40 cells evaluated for each separate independent experiment). Scale bar = 5 μm. A P-value < 0.05(*) was deemed significant. Graph displays median, +/−interquartile range.

39% longer [$P < 0.001$(***)] (median value: 2.53 μm; variation 0.75–7.0 μm) or MCP-1, 31% longer [$P < 0.01$(**)] (median value: 2.39 μm; variation 1.04–6.17 μm).

Previous reports have indicated that cilia can align in the direction of migration, as observed when confluent cancer cells migrated into space during a scratch wound assay (Jones et al., 2012; Schneider et al., 2010). We therefore examined the effect of chemotactic migration on BMSC primary cilia orientation, as determined using a simple orientation scheme (Fig. 5A). Surprisingly, primary cilia did not align to the direction of either FCS or MCP-1 stimulated migration, irrespective of oxygen tension (Figs. 5B–C). However, under hypoxic conditions, using the microtubule organizing center (MTOC) as an indicator of cell polarity, we did observe a significant [$P < 0.05$(*)] increase in the number of BMSCs orientating their MTOC towards the direction of FCS-stimulated migration (Fig. 5D—hatched bars). In addition, MCP-1 mediated chemoattraction induced a noticeable increase in forward orientated MTOC, however this did not reach statistical significance.

Bioinformatic analysis of migration and ciliation signaling pathways

To further investigate how pathways affecting migration may affect cilia, we used computational network modeling to discover connections between the pathways and key proteins linking these processes. We examined the connections between proteins involved in ciliation, centrosome biogenesis, migration and cell cycle using two graph theory measures of network analysis, closeness (Fig. 6A) and betweenness (Fig. S5A) centrality. We found that the modeled pathways were closely linked, as demonstrated by the dense, tightly grouped visual analysis produced. From our analysis we produced a list of key proteins predicted to connect the pathways (Fig. 6B). HSP90aa1, which scored highly on measures of both closeness and betweenness centrality, was chosen for further investigation.

HSP90 inhibition induces ciliation in untreated BMSCs and reduces SFM-stimulated ciliation

We chose to investigate the role of HSP90 using the specific HSP90aa1 inhibitor, AUY922. AUY922 inhibits HSP90α and β subunits at low nano-molar concentrations (Garon et al., 2013) and also leads to inhibition of IKK and phosphatidylinositide 3-kinase (PI3K) signaling pathways (Walsby et al., 2013). As seen previously (Fig. 1B) treatment with 24 h of SFM under normoxic conditions induced a significant [$P < 0.05$(*)] induction in ciliation. Under normoxic oxygen tension with normal growth conditions, AUY922 treatment resulted in a significant [$P < 0.05$(*)] 53% increase in the number of ciliated cells [56% (±11%) compared to 86% (±5.2%)] (Fig. 6C). Under hypoxic oxygen tension the same upward trend in ciliation was observed following AUY922 treatment, however this was not statistically significant.

HSP90 differentially regulates cilia length, subject to oxygen tension

To further explore the effects of HSP90 inhibition, we examined the length of the cilia present following AUY922 treatment (Fig. S5B). Examining the effects under normoxic oxygen tension, as

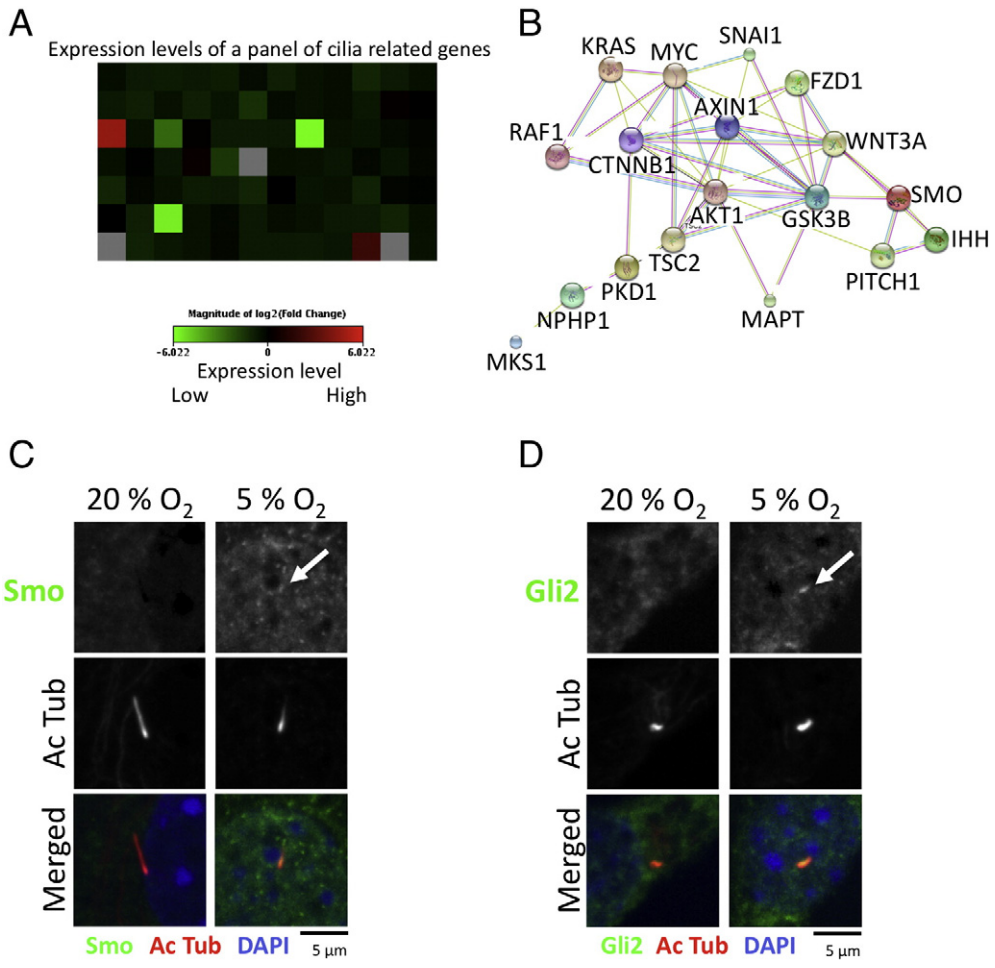

Figure 3 Effects of hypoxia on cilia specific genes. A. Heat map of hypoxia induced changes in cilia related genes. Visualization of hypoxia induced changes (>2 fold) in expression of 86 cilia related genes. B. STRING visualization of links between downregulated genes. Gli2 (green) (C.) and Smo (green) (D.) re-localize to cilia in BMSCs grown under 5% O_2. C–D. Cilia visualized by staining with acetylated α-Tubulin (red). DNA stained with DAPI (blue). Scale bar = 5 μm.

previously observed (Fig. 1C), SFM treatment induced a very significant [$P < 0.01$(**)] increase (25%) in cilia length (median values: 2.0 compared to 2.5 μm; variations 0.4–9.0 and 0.7–5.0 μm respectively). However, the combination of AUY922 and SFM treatment under normoxic oxygen tension, resulted in a significant [$P < 0.01$(**)] reduction (21%) in cilia length (median value 1.68 μm; variation 0.50–5.06 μm), compared to the AUY922 treated control (median value 2.12 μm; variation 0.44–6.87 μm). Furthermore, a significant [$P < 0.001$(***)] reduction in length (33%) was observed following the combination of AUY922 and SFM treatments (median value 1.68 μm), compared to SFM treatment alone (median value 2.5 μm; variation 0.70–5.00 μm) (Fig. 6D). Interestingly, under hypoxic oxygen tension AUY922 treatment resulted in a highly significant [$P < 0.001$(***)] increase (56%) in cilia length in untreated control cells (median value: 2.96; variation 0.55–8.19 μm) compared to AUY922 alone (median value 1.9 μm; variation 0.6–5.4 μm) treated cells. There was a highly significant increase [$P < 0.001$(***)] (41%) in cilia length in control AUY992 treated cells (median value 2.96 μm; variation 0.55–8.19 μm) compared to SFM treated cells (median value 2.1 μm; variation 0.50–8.6 μm). Furthermore, under hypoxic conditions AUY922 treatment combined with SFM resulted in a significant [$P < 0.001$(***)] decrease (33%) in cilia length (median value 1.98 μm; variation 0.44–7.27 μm), compared to the AUY922 alone (median value 2.96 μm; variation 0.56–8.19 μm) treated cells (Fig. 6 D). Strikingly, comparing between oxygen tensions AUY922 treatment alone resulted in a highly significant [$P < 0.001$(***)] increase (41%) in cilia length in BMSCs grown under hypoxia (median value 2.96 μm; variation 0.56–8.19 μm), compared to normoxia (median value 2.1 μm; variation 0.44–6.87 μm).

PI3K inhibition increases ciliation and cilia length

As HSP90 inhibition is reported to affect the PI3K signaling pathway (Walsby et al., 2013), we directly inhibited this pathway using the PI3K inhibitor LY-294002 and examined the effects on BMSC cilia (Fig. 7). Cilia present on cells treated with LY-294002 appeared noticeably thinner and were more weakly stained by acetylated α-Tubulin (Fig. S5C). Under

Table 1 Significant changes in gene expression stimulated by hypoxic growth conditions. Left column: Gene name and fold (>2) changes in gene expression in BMSCs grown under 5% O_2, compared to 20% O_2. BMSC serum-starved for 24 h to induce ciliation. N = 2. Right column: Gene function.

Gene symbol	Fold regulation	Gene function
Genes up-regulated		
Fos	23.8762	Regulator of cell proliferation, differentiation, and transformation.
Vangl2	4.1626	Wnt signaling, regulation of planar cell polarity, facial branchiomotor neuron migration.
Genes down-regulated		
Bbs1	−2.1697	Formation and function of ciliary gate; Hedgehog signaling
Cdk5rap2	−2.6344	Localized to the centrosome and Golgi complex, CDK5R1 and pericentrin (PCNT), plays a role in centriole engagement and microtubule nucleation.
Fzd-1	−7.1478	Receptor for Wnt signaling proteins
Gsk3b	−65.006	Involved in Wnt signaling and regulation of transcription factors and microtubules. Regulates cilia length.
Ihh	−3.0367	Binding of Ihh to its receptor Patched (Ptc) allows Smo to initiate the signaling cascade that leads to activation of the Cubitus interrupts (Ci) transcription factor family members Gli1, Gli2, and Gli3
Kras	−2.1772	Induces or enhances Shh expression. Interferes with Gli2 function and Gli3 processing.
Mks1	−2.1622	Formation and function of ciliary gate; Hedgehog signaling Regulates cilia length through Shh and Gli3 regulation
Nphp1	−2.0813	Formation and function of ciliary gate
Pkd1	−50.1264	Membrane-spanning protein that localizes to the centrosome and cilium in renal epithelial cells, and work in a complex to sense ciliary bending
Rock2	−2.1251	Stabilizing the actin cytoskeleton and cell adhesion.
Smo	−2.0527	G protein-coupled receptor that interacts with the patched protein (PTCH) to transduce hedgehog signaling. Required for the accumulation of KIF7 and GLI3 in the cilia

normoxic conditions we found that combining LY-294002 treatment with SFM resulted in a significant [$P < 0.05$(*)] 33% increase in the number of ciliated cells [88% (±9%)], compared to untreated controls [66% (±14.5%)] (Fig. 7A, left side of panel). In addition, under hypoxic conditions, the combination of LY-294002 and SFM treatments induced a very significant [$P < 0.01$(**)] 42% increase in the number of ciliated cells [94% (±5%)], compared to the hypoxic untreated control [66% (±14%)] (Fig. 7A, right side of panel). Statistical analysis revealed no further significant effects of LY-294002 treatment on ciliation.

Under normoxic conditions the combination of LY-294002 and SFM treatments resulted in a significant [$P < 0.05$(*)] 22% increase in cilia length (median value 2.29 μm; variation 0.50–8.96 μm), compared to LY-294002 treatment alone (median value 1.87 μm; variation 0.56–9.81 μm) (Fig. 7B). Investigating the effect of LY-294002 treatment on cilia length, under normoxic conditions we found a significant [$P < 0.001$(***)] 9% decrease in cilia length following the combination of LY-294002 and SFM treatments (median value 2.29 μm; variation 0.50–8.96 μm), compared to SFM treatment alone (median value 2.5 μm; variation 0.70–5.0 μm). Conversely, under hypoxic conditions we found that the combination of LY-294002 and SFM resulted in a highly significant [$P < 0.001$(***)] 31% increase in cilia length (median value 2.75 μm; variation 0.50–7.52 μm), compared to SFM alone (median value 2.1 μm; variation 0.50–8.60 μm) (Fig. 7B). Similar to normoxia, under hypoxic conditions combining SFM with LY-294002 treatment resulted in a very significant [$P < 0.01$(**)] 28% increase in cilia length (median value 2.75 μm; variation 0.50–7.52 μm), compared to LY-294002 alone (median value 2.15 μm; variation 0.42–7.10 μm) (Fig. 7B).

Discussion

We found that primary BMSCs adapt to a hypoxic environment by regulating cilia length. Additionally, we found that key components of the Hedgehog signaling pathway are down-regulated in BMSCs constitutively exposed to hypoxic conditions and that this resulted in changes to the recruitment of proteins to the cilia. Furthermore, using pathway modeling we illuminated and validated HSP90 and PI3K signaling as regulating cilia length in BMSCs.

Our results indicate that under hypoxic conditions ~50% of the cell population is cycling, compared to ~20% under normoxic conditions, supporting a previous report that hypoxia induces BMSC proliferation (Berniakovich and Giorgio, 2013). Although acute changes in oxygen tension have important consequences for BMSC function, currently there are no reports directly investigating how chronic exposure to hypoxia affects BMSC cilia. Our results indicate that cycling hypoxic BMSC cultures contain cilia that are significantly longer than BMSCs grown under normoxia (Fig. 1C). Supporting our results, it has previously been reported that acute exposure of normoxic cell cultures to the hypoxia mimetics cobalt chloride (Verghese et al., 2011) or DMOG (Wann et al., 2013) results in an increase in cilia length. The significant decrease in cilia

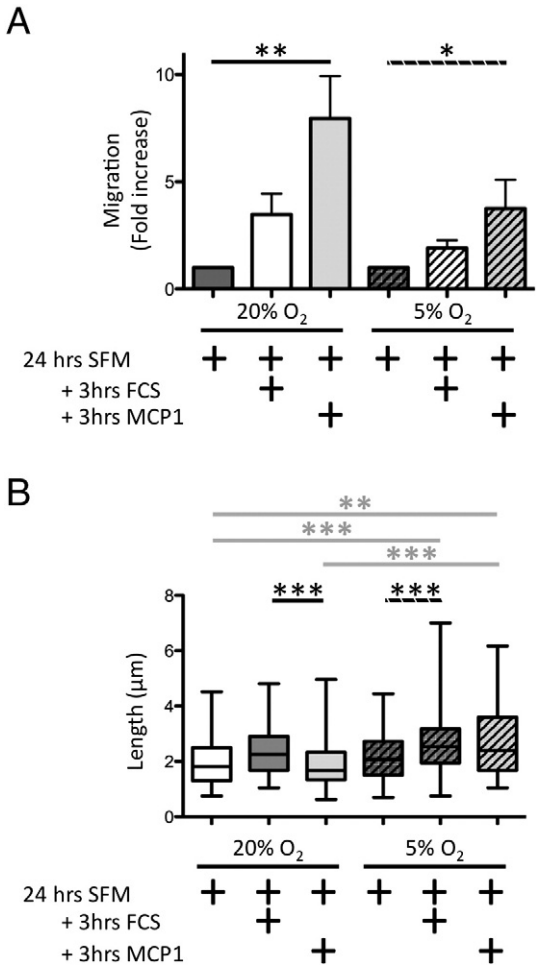

Figure 4 Differential effects of O_2 tension and chemoattractant on migrating BMSC cilia length. A. Normalized, fold increase of chemotactically stimulated (as indicated) migrating BMSC under 20% O_2 (left) or 5% O_2 (right) tension. Graph represents N = 3 (>100 cells evaluated for each separate independent experiment). B. Cilia length in BMSCs migrating in response to indicated chemoattractant, under 20% (left) or 5% (right) O_2 tension. Graph represents N = 3 (>50 cilia evaluated for each separate independent experiment). A P-value <0.05(*) was deemed significant, $P < 0.01$(**) very significant, and a $P < 0.001$(***) highly significant. Graph displays median, +/−interquartile range and maximum and minimum measurements.

length observed under normoxic conditions and following 48 h SFM treatment is likely due to the prolonged lack of nutrients affecting energy intensive cellular processes as cilia are dynamic, requiring energy for maintenance. However, further work is needed to confirm this. As previously reported, we found that subjecting primary BMSCs to serum starvation led to cell cycle arrest (McMurray et al., 2013). We found that serum starvation of BMSCs results in a significant increase in cilia length under normoxic conditions, likely resulting from their enforced accumulation in the G_0 cell cycle phase (Fig. S2). This would favor signaling for cilia assembly, in the absence of cell cycle signaling, resulting in longer cilia. Our primary BMSC cultures contained low, persistent levels of centrosome amplification that were unchanged by any conditions tested (Fig. 2B), consistent with levels reported in other cell culture systems (Holubcová et al., 2011; Tarapore et al., 2001). However, we observed a significant increase in twin γ-Tubulin foci stimulated by 24 h of SFM treatment under normoxic conditions, which may indicate an increased level of centrosome splitting (Fig. 2C). This supports a previous report, using hTERT-RPE1 cells, that SFM treatment induces centrosome splitting (Graser et al., 2007). These results highlight the importance of understanding the effects of chronic hypoxia exposure on BMSCs, which is the physiologically relevant environment for these cells. This stands in contrast to the commonly investigated affects of acute exposure to hypoxia or hypoxia mimetic drugs, on normoxic cultured BMSCs. To underscore the importance of understanding how different environments affect cells, a recent report highlighted the effects of differing microenvironments on cell populations residing in distinctive niches within the bone marrow compartment (Wang et al., 2012).

To further understand how chronic hypoxia affects BMSCs we identified down-regulation of genes involved in Wnt (Fzd-1, Bbs1, GSK3β, Smo) and Hh (Ihh, Smo) signaling (Table 1) (Barakat et al., 2013). Interestingly, we observed up-regulation of Vangl2, which is involved in the non-canonical Wnt pathway and migration (Ross et al., 2005). As previously reported, these changes in gene expression likely reflect a change in the differentiation potential of BMSCs grown under hypoxic conditions (Drela et al., 2014; Fehrer et al., 2007). In addition to the hypoxic down-regulation of Smo transcripts, we observed that hypoxia mediated the re-localization of Smo proteins to the cilia (Fig. 3C). Furthermore, hypoxia induced Gli2, a target of many of the down-regulated genes, to re-localize to the cilia (Fig. 3D). Additionally, Gli2 and Smo ciliary re-localization has been observed in response to the de-regulation of ciliary calcium levels (Delling et al., 2013). Supporting our findings, it was observed that alterations in Smo and Gli2 levels accompanied changes in cilia length (Nathwani et al., 2014). Future work will be required to determine if long-term exposure to hypoxia alters expression of Hh targets, such as Ptch and Gli1. Ihh and Smo have previously been implicated in signal transduction in chondrocytes (Shao et al., 2012), suggesting that cilia related signaling and hypoxia could influence BMSC differentiation decisions. Indeed previous work has indicated that the long-term culture of BMSCs under hypoxic conditions supports BMSCs retaining an undifferentiated state (Basciano et al., 2011; Berniakovich and Giorgio, 2013). Many of the genes we identified as down-regulated are linked to cell cytoskeleton re-organization, which is required for differentiation (Müller et al., 2013) and motility/migration (Antoniades et al., 2014; Döppler et al., 2013; Fong et al., 2009; Ishizuka et al., 2011; Kulaga et al., 2004; Laeremans et al., 2010; Lin et al., 2012; Lock et al., 2012; Shinozaki et al., 2008). Consistent with this, it has been reported that under normoxic conditions ROCK inhibition increases ciliation and cilia length (Hernandez-Hernandez et al., 2013; McMurray et al., 2013) as does inhibition of F-actin (Yan and Zhu, 2012), both of which mimic the effects we observed under hypoxia. Together with our data this suggests that the differentiation potential of BMSCs will be, at least partially, dependent upon the oxygen tension in which the cells are cultured and that cilia may play an important role in this decision.

Investigating the effects of chemotactic-mediated migration, under different oxygen tensions, on BMSC cilia we found that the cilia of sub-confluent primary BMSCs did not

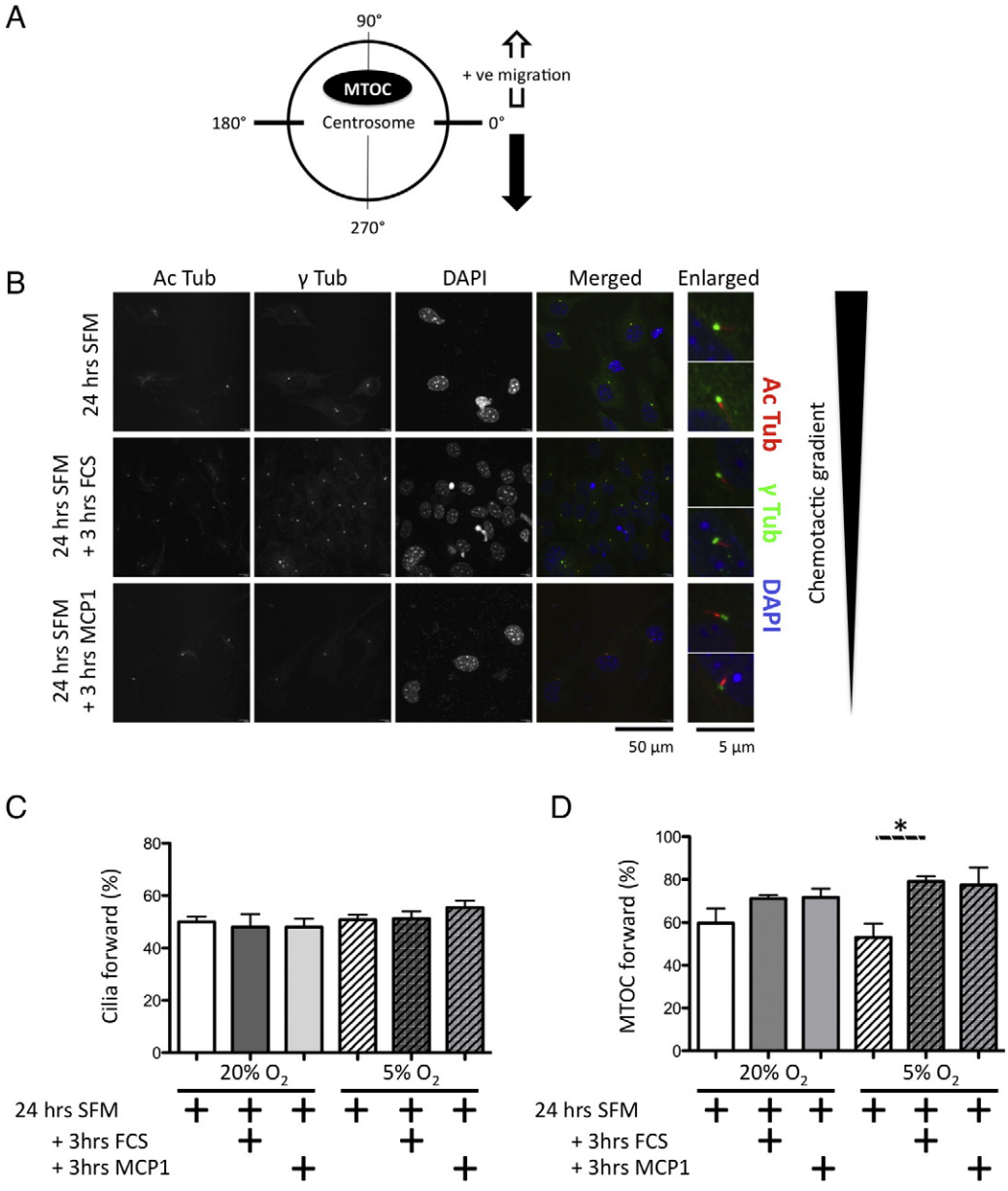

Figure 5 Chemotactic induced migration of BMSCs. A. Template used to determine cilia orientation. Cilia orientation measured from base (centrosome) to cilia tip. B. Immunofluorescent visualization of cilia. Cilia visualized by staining with acetylated α-Tubulin (red). Centrosomes visualized by staining for γ-Tubulin (green). DNA stained with DAPI (blue). Scale bar = 50 μm or 5 μm, as indicated. C. Percentage of migrating BMSCs with the cilia orientated towards chemotactic stimulus (as determined using scheme A), following the indicated treatments. Graph represents N = 3 (>50 cells evaluated for each separate independent experiment). D. Percentage of migrating BMSC with the MTOC orientated towards the direction of chemotactic migration, following the indicated treatments. Graph represents N = 3 (~50 cells evaluated for each separate independent experiment). Students *T* test, two tailed. A P-value <0.05 (*) was deemed significant.

align to the direction of chemotactic migration (Fig. 5C). Cilia can align to the direction of migration, however this was reported using confluent cancer cells migrating into space, via a scratch wound assay (Jones et al., 2012; Schneider et al., 2010). We found that oxygen tension did markedly effect chemotactic-mediated BMSC migration, however this did not reach statistical significance (Fig. 4A). The reduction in migration observed under hypoxic conditions, in conjunction with our gene expression data and the re-localization of Smo and Gli, supports a recent report which indicated that Smo localization and down-regulation of the Gli transcription factors can affect migration (Chen et al., 2014; Lin et al., 2012). Notably, supporting our gene expression data (Fig. 3A), we did find that the combination of hypoxia and migration significantly affected the length of cilia (Fig. 4B). The longer cilia observed in migrating BMSCs is likely linked to the process of actin polymerization required for the movement of migrating of cells, however further work will be required to assess this. Together, this suggests that the mechanisms governing cilia length and

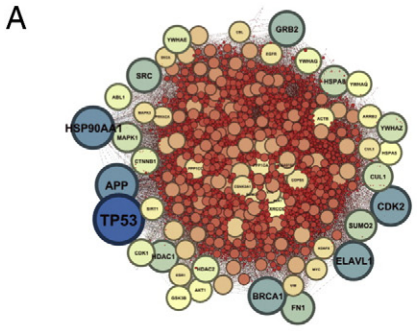

B

Rank	Rank-Betweeness	Rank-Closeness
	Protein or Gene Name	
1	APP	ELAVL1
2	ELAVL1	APP
3	TP53	TP53
4	HSP90AA1	HSP90AA1
5	FN1	CDK2
6	GRB2	GRB2
7	SUMO2	SRC
8	SRC	FN1
9	BRCA1	SUMO2
10	CDK2	CDK1

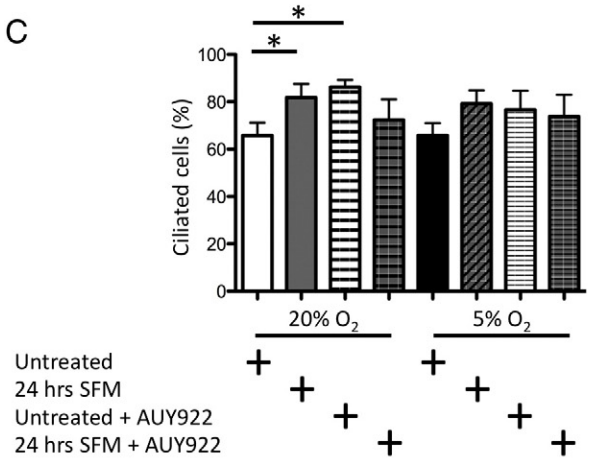

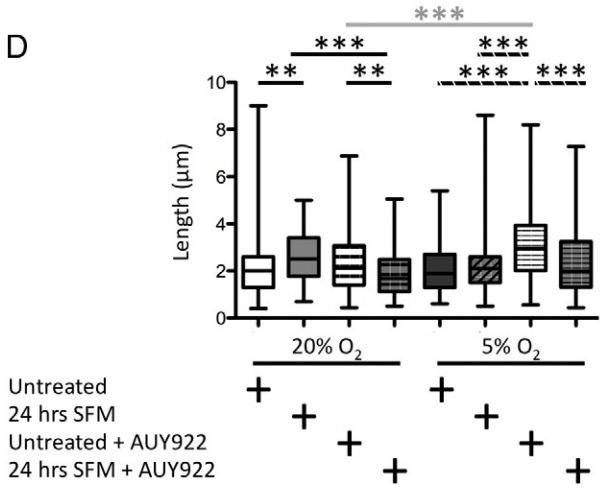

Figure 6 Predicting and validating proteins linking ciliation and migration. A. Eigenvector centrality (closeness) as a measure of approximate importance of each node in the network. Node size proportional to its centrality/importance. B. Top 10 ranked proteins as measured using indicated centrality measure. C. HSP90 inhibition affects ciliation. 24 h treatment with 100 nM AUY922 significantly affects ciliation, under 20% (left) O_2 tension but not 5% O_2 tension (right) D. AUY922 (100 nM) significantly affects cilia length under 20% (left) and 5% (right) O_2 tension. A P-value <0.05(*) was deemed significant, $P < 0.01$(**) very significant, and a $P < 0.001$(***) highly significant. Graph represents N = 3 (>40 cilia evaluated for each separate independent experiment). Graph displays median, +/− interquartile range and maximum and minimum measurements.

migration are linked and can be influenced by oxygen tension. Exploring this, our network modeling elucidated links between the ciliation and migration pathways, identifying key proteins potentially linking the two processes (Fig. 6B). We validated our modeling using a key protein identified, HSP90, which has previously been localized to cilia and linked to heat shock induced cilia shortening (Prodromou et al., 2012). Inhibition of HSP90 (by AUY922) under normoxia and normal growth conditions significantly increased the number of ciliated cells (Fig. 6C). Supporting this, it has previously been shown that the inhibition of HSP90 leads to a G_1 arrest (Georgakis et al., 2006), which

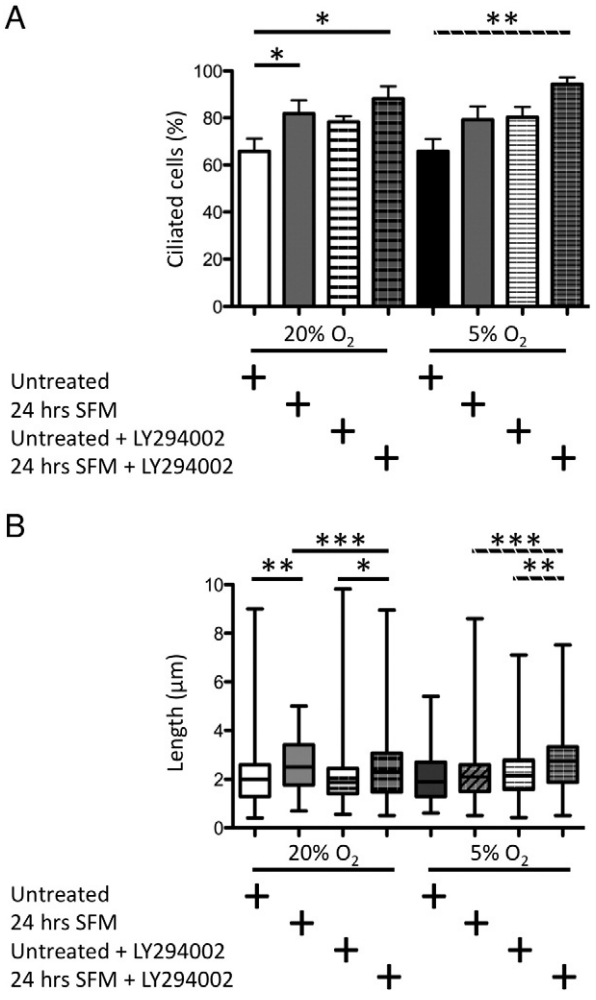

Figure 7 PI3K inhibition affects cilia numbers and length. BMSCs were treated with LY-294002 under the indicated conditions for 24 h. A. 5 μM LY-294002 treatment, under 20% O_2 (left) or 5% O_2 (right) induces ciliation. B. 5 μM LY-294002 significantly increases cilia length following SFM treatment under 20% O_2 (left) or 5% O_2 (right). Graph represents N = 3 (>40 cilia evaluated for each separate independent experiment). A P-value < 0.05(*) was deemed significant, P < 0.01(**) very significant, and a P < 0.001(***) highly significant. Graph displays median, +/− interquartile range and maximum and minimum measurements.

would increase ciliation. Interestingly, we found that AUY922 treatment had inverse, oxygen tension-dependent effects on cilia length and we speculate that this is due to different, oxygen tension-dependent, targets of HSP90. Supporting this, oxygen tension-dependent effects of AUY922 on the actin cytoskeleton, cytoskeleton dependent signaling and stress signaling pathways have previously been reported (Djuzenova et al., 2012; Hartmann et al., 2013; Schilling et al., 2012). Specifically we found that primary BMSCs respond to HSP90 inhibition, while previous reports indicate that chondrocytes do not (Wann et al., 2013). This suggests that differentiation may affect cilia related signaling. Interestingly, chronic HSP90 inhibition may promote BMSC differentiation (van der Kraan et al., 2013). However further work is needed to determine if long-term hypoxia exposure, which supports an undifferentiated state (Basciano et al., 2011; Berniakovich and Giorgio, 2013), influences the differentiation potential of BMSCs.

To further investigate the HSP90 signaling pathway we inhibited the downstream molecule PI3K, which is involved in cell migration and basal body signaling (Fukata et al., 2003; Yoneda et al., 2005; Zhu et al., 2009b). Migration signaling involves the Rac GTPase interacting protein, which has been implicated in cilia elongation (Kim et al., 2010). Our data supported this as PI3K inhibition, alone or in combination with SFM treatment, resulted in increases in ciliation (Fig. 7A) and significantly affected cilia length. Interestingly, combining PI3K inhibition with SFM treatment produced effects that were oxygen tension dependent (Fig. 7B). Overall the effect of inhibitors used in this study produced small but significant changes in cilia length, comparable to other reports (Ghossoub et al., 2013; Hori et al., 2014; Prodromou et al., 2012; Wann et al., 2013; Yang et al., 2013).

Our results significantly enhance the current understanding of how BMSCs adapt and respond to chronic exposure to hypoxic oxygen tension, advancing our knowledge regarding key, fundamental aspects of BMSC biology. Understanding how oxygen tension affects cultured primary BMSCs has direct repercussions, likely affecting their therapeutic efficacy. Our findings are paving the way for researchers to fully exploit the next generation of stem cell-based regenerative medicine therapies through manipulation of cilia-related signaling pathways, potentially leading to improvements in stem cell homing and engraftment.

Author contributions

JALB: conceived the project, designed experiments, acquired the data, analyzed and interpreted data, wrote the manuscript, and had final approval of the manuscript. TS: performed the computational modeling analysis. PO: provided access to facilities and essential software. FB: financial support, edited the manuscript, final approval of manuscript.

Supplementary data to this article can be found online at http://dx.doi.org/10.1016/j.scr.2014.06.006.

Acknowledgments

JALB and TS are funded by Systems Biology Ireland through Science foundation Ireland grant 06/CE/B1129. We would like to thank Professor Ciaran Morrison (Centre for Chromosome Biology) for the gift of Smo and Gli2 antibodies, Dr Aline Morrison (REMEDI) for providing the BMSCs and Dr Shirley Hanley (REMEDI) for the assistance with FACS. We would also like to thank Dr Róisín Dwyer and Dr Emer Bourke for critical discussion of the manuscript.

References

Alibés, A., Yankilevich, P., Cañada, A., Díaz-Uriarte, R., 2007. IDconverter and IDClight: conversion and annotation of gene and protein IDs. BMC Bioinform. 8, 9.

Antoniades, I., Stylianou, P., Skourides, P.A., 2014. Making the connection: ciliary adhesion complexes anchor basal bodies to the actin cytoskeleton. Dev. Cell 28 (1), 70–80.

Arnaiz, O., Malinowska, A., Klotz, C., Sperling, L., Dadlez, M., Koll, F., Cohen, J., 2009. Cildb: a knowledgebase for centrosomes and cilia. Database (Oxford) bap022.
Avasthi, P., Marshall, W.F., 2012. Stages of ciliogenesis and regulation of ciliary length. Differentiation 83, S30–S42.
Azimzadeh, J., Marshall, W.F., 2010. Building the centriole. Curr. Biol. 20, R816–R825.
Bader, G.D., Betel, D., Hogue, C.W., 2003. BIND: the biomolecular interaction network database. Nucleic Acids Res. 31, 248–250.
Barakat, B., Yu, L., Lo, C., Vu, D., De Luca, E., Cain, J.E., Martellotto, L.G., Dedhar, S., Sadler, A.J., Wang, D., 2013. Interaction of smoothened with integrin-linked kinase in primary cilia mediates Hedgehog signalling. EMBO Rep. 14, 837–844.
Basciano, L., Nemos, C., Foliguet, B., de Isla, N., de Carvalho, M., Tran, N., Dalloul, A., 2011. Long term culture of mesenchymal stem cells in hypoxia promotes a genetic program maintaining their undifferentiated and multipotent status. BMC Cell Biol. 12, 12.
Basten, S.G., Giles, R.H., 2013. Functional aspects of primary cilia in signaling, cell cycle and tumorigenesis. Cilia 2, 6.
Berg, H.C., Purcell, E.M., 1977. Physics of chemoreception. Biophys. J. 20, 193–219.
Berniakovich, I., Giorgio, M., 2013. Low oxygen tension maintains multipotency, whereas normoxia increases differentiation of mouse bone marrow stromal cells. Int. J. Mol. Sci. 14, 2119–2134.
Bialek, W., Setayeshgar, S., 2005. Physical limits to biochemical signaling. Proc. Natl. Acad. Sci. U. S. A. 102, 10040–10045.
Bornens, M., 2012. The centrosome in cells and organisms. Science 335, 422–426.
Bourke, E., Brown, J.A.L., Takeda, S., Hochegger, H., Morrison, C. G., 2010. DNA damage induces Chk1-dependent threonine-160 phosphorylation and activation of Cdk2. Oncogene 29, 616–624.
Branzei, D., Foiani, M., 2008. Regulation of DNA repair throughout the cell cycle. Nat. Rev. Mol. Cell Biol. 9, 297–308.
Brown, J.A.L., Bourke, E., Liptrot, C., Dockery, P., Morrison, C.G., 2010. MCPH1/BRIT1 limits ionizing radiation-induced centrosome amplification. Oncogene 29 (40), 5537–5544.
Brown, J.A.L., Roberts, T.L., Richards, R., Woods, R., Birrell, G., Lim, Y.C., Ohno, S., Yamashita, A., Abraham, R.T., Gueven, N., et al., 2011. A novel role for hSMG-1 in stress granule formation. Mol. Cell. Biol. 31 (22), 4417–4429.
Chen, Q., Xu, R., Zeng, C., Lu, Q., Huang, D., Shi, C., Zhang, W., Deng, L., Yan, R., Rao, H., et al., 2014. Down-regulation of Gli transcription factor leads to the inhibition of migration and invasion of ovarian cancer cells via integrin β4-mediated FAK signaling. PLoS ONE 9, e88386.
Christensen, S.T., Pedersen, S.F., Satir, P., Veland, I.R., Schneider, L., 2008. The primary cilium coordinates signaling pathways in cell cycle control and migration during development and tissue repair. Curr. Top. Dev. Biol. 85, 261–301.
Davenport, J.R., Yoder, B.K., 2005. An incredible decade for the primary cilium: a look at a once-forgotten organelle. Am. J. Physiol. Renal Physiol. 289, F1159–F1169.
Delling, M., DeCaen, P.G., Doerner, J.F., Clapham, S.F.D.E., 2013. Primary cilia are specialized calcium signalling organelles. Nature 504, 311–314.
Dinkel, H., Chica, C., Via, A., Gould, C.M., Jensen, L.J., Gibson, T. J., Diella, F., 2011. Phospho. ELM: a database of phosphorylation sites—update 2011. Nucleic Acids Res. 39, D261–D267.
Djuzenova, C.S., Blassl, C., Roloff, K., Kuger, S., Katzer, A., Niewidok, N., Günther, N., Polat, B., Sukhorukov, V.L., Flentje, M., 2012. Hsp90 inhibitor NVP-AUY922 enhances radiation sensitivity of tumor cell lines under hypoxia. Cancer Biol. Ther. 13, 425–434.
Döppler, H., Bastea, L.I., Eiseler, T., Storz, P., 2013. Neuregulin mediates F-actin-driven cell migration through inhibition of protein kinase D1 via Rac1 protein. J. Biol. Chem. 288, 455–465.
Drela, K., Sarnowska, A., Siedlecka, P., Szablowska-Gadomska, I., Wielgos, M., Jurga, M., Lukomska, B., Domanska-Janik, K., 2014. Low oxygen atmosphere facilitates proliferation and maintains undifferentiated state of umbilical cord mesenchymal stem cells in an hypoxia inducible factor-dependent manner. Cytotherapy 6 (7), 881–892.
Fehrer, C., Brunauer, R., Laschober, G., Unterluggauer, H., Reitinger, S., Kloss, F., Gülly, C., Gaßner, R., Lepperdinger, G., 2007. Reduced oxygen tension attenuates differentiation capacity of human mesenchymal stem cells and prolongs their lifespan. Aging Cell 6, 745–757.
Fong, K.-W., Hau, S.-Y., Kho, Y.-S., Jia, Y., He, L., Qi, R.Z., 2009. Interaction of CDK5RAP2 with EB1 to track growing microtubule tips and to regulate microtubule dynamics. Mol. Biol. Cell 20, 3660–3670.
Fukata, M., Nakagawa, M., Kaibuchi, K., 2003. Roles of Rho-family GTPases in cell polarisation and directional migration. Curr. Opin. Cell Biol. 15, 590–597.
Ganem, N.J., Godinho, S.A., Pellman, D., 2009. A mechanism linking extra centrosomes to chromosomal instability. Nature 460, 278–282.
Garon, E.B., Finn, R.S., Hamidi, H., Dering, J., Pitts, S., Kamranpour, N., Desai, A.J., Hosmer, W., Ide, S., Avsar, E., et al., 2013. The HSP90 inhibitor NVP-AUY922 potently inhibits non-small cell lung cancer growth. Mol. Cancer Ther. 12 (6), 890–900.
Georgakis, G.V., Li, Y., Younes, A., 2006. The heat shock protein 90 inhibitor 17-AAG induces cell cycle arrest and apoptosis in mantle cell lymphoma cell lines by depleting cyclin D1, Akt, Bid and activating caspase 9. Br. J. Haematol. 135, 68–71.
Ghossoub, R., Hu, Q., Failler, M., Rouyez, M.-C., Spitzbarth, B., Mostowy, S., Wolfrum, U., Saunier, S., Cossart, P., JamesNelson, W., et al., 2013. Septins 2, 7 and 9 and MAP4 colocalize along the axoneme in the primary cilium and control ciliary length. J. Cell Sci. 126, 2583–2594.
Gotlieb, A.I., Subrahmanyan, L., Kalnins, V.I., 1983. Microtubule-organizing centers and cell migration: effect of inhibition of migration and microtubule disruption in endothelial cells. J. Cell Biol. 96, 1266–1272.
Graser, S., Stierhof, Y.-D., Lavoie, S.B., Gassner, O.S., Lamla, S., Le Clech, M., Nigg, E.A., 2007. Cep164, a novel centriole appendage protein required for primary cilium formation. J. Cell Biol. 179, 321–330.
Han, Y.-G., Spassky, N., Romaguera-Ros, M., Garcia-Verdugo, J.-M., Aguilar, A., Schneider-Maunoury, S., Alvarez-Buylla, A., 2008. Hedgehog signaling and primary cilia are required for the formation of adult neural stem cells. Nat. Neurosci. 11, 277–284.
Hartmann, S., Günther, N., Biehl, M., Katzer, A., Kuger, S., Worschech, E., Sukhorukov, V.L., Krohne, G., Zimmermann, H., Flentje, M., et al., 2013. Hsp90 inhibition by NVP-AUY922 and NVP-BEP800 decreases migration and invasion of irradiated normoxic and hypoxic tumor cell lines. Cancer Lett. 331, 200–210.
Hernandez-Hernandez, V., Pravincumar, P., Diaz-Font, A., May-Simera, H., Jenkins, D., Knight, M., Beales, P.L., 2013. Bardet–Biedl syndrome proteins control the cilia length through regulation of actin polymerization. Hum. Mol. Genet. 22, 3858–3868.
Hoey, D.A., Tormey, S., Ramcharan, S., O'brien, F.J., Jacobs, C.R., 2012. Primary cilia-mediated mechanotransduction in human mesenchymal stem cells - Hoey-2012—STEM CELLS — Wiley Online Library. Stem Cells 30, 2561–2570.
Holubcová, Z., Matula, P., Sedláčková, M., Vinarský, V., Doležalová, D., Bárta, T., Dvořák, P., Hampl, A., 2011. Human embryonic stem cells suffer from centrosomal amplification — Holubcová-2011 — STEM CELLS — Wiley Online Library. J. Cell. Physiol. 29, 46–56.
Hori, A., Ikebe, C., Tada, M., Toda, T., 2014. Msd1/SSX2IP-dependent microtubule anchorage ensures spindle orientation and primary cilia formation. EMBO Rep. 15 (2), 175–184.
Hornbeck, P.V., Kornhauser, J.M., Tkachev, S., Zhang, B., Skrzypek, E., Murray, B., Latham, V., Sullivan, M., 2012. PhosphoSitePlus: a comprehensive resource for investigating the structure and function of experimentally determined post-translational modifications in man and mouse. Nucleic Acids Res. 40, D261–D270.

Ishikawa, H., Thompson, J., Yates, J.R., Marshall, W.F., 2012. Proteomic analysis of mammalian primary cilia. Curr. Biol. 22, 414–419.

Ishizuka, K., Kamiya, A., Oh, E.C., Kanki, H., Seshadri, S., Robinson, J.F., Murdoch, H., Dunlop, A.J., Kubo, K.-I., Furukori, K., et al., 2011. DISC1-dependent switch from progenitor proliferation to migration in the developing cortex. Nature 473, 92–96.

Jones, T.J., Adapala, R.K., Geldenhuys, W.J., Bursley, C., AbouAlaiwi, W.A., Nauli, S.M., Thodeti, C.K., 2012. Primary cilia regulates the directional migration and barrier integrity of endothelial cells through the modulation of hsp27 dependent actin cytoskeletal organization. J. Cell. Physiol. 227, 70–76.

Kim, J., Lee, J.E., Heynen-Genel, S., Suyama, E., Ono, K., Lee, K., Ideker, T., Aza-Blanc, P., Gleeson, J.G., 2010. Functional genomics screen for modulators of ciliogenesis and cilium length. Nature 464, 1048–1051.

Kulaga, H.M., Leitch, C.C., Eichers, E.R., Badano, J.L., Lesemann, A., Hoskins, B.E., Lupski, J.R., Beales, P.L., Reed, R.R., Katsanis, N., 2004. Loss of BBS proteins causes anosmia in humans and defects in olfactory cilia structure and function in the mouse. Nat. Genet. 36, 994–998.

Laeremans, H., Rensen, S.S., Ottenheijm, H.C.J., Smits, J.F.M., Blankesteijn, W.M., 2010. Wnt/frizzled signalling modulates the migration and differentiation of immortalized cardiac fibroblasts. Cardiovasc. Res. 87, 514–523.

Li, R., Gundersen, G.G., 2008. Beyond polymer polarity: how the cytoskeleton builds a polarized cell. Nat. Rev. Mol. Cell Biol. 9, 860–873.

Lin, C., Nozawa, Y.I., Chuang, P.-T., 2012. The path to chemotaxis and transcription is smoothened. Sci. Signal. 5, pe35.

Lock, F.E., Ryan, K.R., Poulter, N.S., Parsons, M., Hotchin, N.A., 2012. Differential regulation of adhesion complex turnover by ROCK1 and ROCK2. PLoS ONE 7, e31423.

Malone, A.M.D., Anderson, C.T., Tummala, P., Kwon, R.Y., Johnston, T.R., Stearns, T., Jacobs, C.R., 2007. Primary cilia mediate mechanosensing in bone cells by a calcium-independent mechanism. Proc. Natl. Acad. Sci. U. S. A. 104, 13325–13330.

Mardin, B.R., Schiebel, E., 2012. Breaking the ties that bind: new advances in centrosome biology. J. Cell Biol. 197, 11–18.

McMurray, R.J., Wann, A.K.T., Thompson, C.L., Connelly, J.T., Knight, M.M., 2013. Surface topography regulates wnt signaling through control of primary cilia structure in mesenchymal stem cells. Sci. Rep. 3, 3545.

Müller, P., Langenbach, A., Kaminski, A., Rychly, J., 2013. Modulating the actin cytoskeleton affects mechanically induced signal transduction and differentiation in mesenchymal stem cells. PLoS ONE 8, e71283.

Nathwani, B.B., Miller, C.H., Yang, T.-L.T., Solimano, J.L., Liao, J.-C., 2014. Morphological differences of primary cilia between human induced pluripotent stem cells and their parental somatic cells. Stem Cells Dev. 23, 115–123.

Nigg, E.A., Raff, J.W., 2009. Centrioles, centrosomes, and cilia in health and disease. Cell 139, 663–678.

Nigg, E.A., Stearns, T., 2011. The centrosome cycle: centriole biogenesis, duplication and inherent asymmetries. Nat. Cell Biol. 13, 1154–1160.

Oh, E.C., Katsanis, N., 2012. Cilia in vertebrate development and disease. Development 139, 443–448.

Opsahl, T., Agneessens, F., Skvoretz, J., 2010. Node centrality in weighted networks: generalizing degree and shortest paths. Soc. Networks 32, 245–251.

Pan, J., Wang, Q., Snell, W.J., 2005. Cilium-generated signaling and cilia-related disorders. Lab. Investig. 85, 452–463.

Petrie, R.J., Doyle, A.D., Yamada, K.M., 2009. Random versus directionally persistent cell migration. Nat. Rev. Mol. Cell Biol. 10, 538–549.

Prasad, T.K., Goel, R., Kandasamy, K., Keerthikumar, S., Kumar, S., Mathivanan, S., Telikicherla, D., Raju, R., Shafreen, B., Venugopal, A., 2009. Human protein reference database—2009 update. Nucleic Acids Res. 37, D767–D772.

Prodromou, N.V., Thompson, C.L., Osborn, D.P.S., Cogger, K.F., Ashworth, R., Knight, M.M., Beales, P.L., Chapple, J.P., 2012. Heat shock induces rapid resorption of primary cilia. J. Cell Sci. 125, 4297–4305.

Proulx-Bonneau, S., Annabi, B., 2011. The primary cilium as a biomarker in the hypoxic adaptation of bone marrow-derived mesenchymal stromal cells: a role for the secreted frizzled-related proteins. 6, 107–118.

Quarmby, L.M., Parker, J.D.K., 2005. Cilia and the cell cycle? J. Cell Biol. 169, 707–710.

Reiter, J.F., Blacque, O.E., Leroux, M.R., 2012. The base of the cilium: roles for transition fibres and the transition zone in ciliary formation, maintenance and compartmentalization. EMBO Rep. 13 (7), 608–618.

Ross, A.J., May-Simera, H., Eichers, E.R., Kai, M., Hill, J., Jagger, D.J., Leitch, C.C., Chapple, J.P., Munro, P.M., Fisher, S., et al., 2005. Disruption of Bardet–Biedl syndrome ciliary proteins perturbs planar cell polarity in vertebrates. Nat. Genet. 37, 1135–1140.

Satir, P., Christensen, S.T., 2007. Overview of structure and function of mammalian cilia. Annu. Rev. Physiol. 69, 377–400.

Satir, P., Pedersen, L.B., Christensen, S.T., 2010. The primary cilium at a glance. J. Cell Sci. 123, 499–503.

Schilling, D., Bayer, C., Li, W., Molls, M., Vaupel, P., Multhoff, G., 2012. Radiosensitization of normoxic and hypoxic h1339 lung tumor cells by heat shock protein 90 inhibition is independent of hypoxia inducible factor-1α. PLoS ONE 7, e31110.

Schmidt, K.N., Kuhns, S., Neuner, A., Hub, B., Zentgraf, H., Pereira, G., 2012. Cep164 mediates vesicular docking to the mother centriole during early steps of ciliogenesis. J. Cell Biol. 199, 1083–1101.

Schneider, L., Cammer, M., Lehman, J., Nielsen, S.K., Guerra, C.F., Veland, I.R., Stock, C., Hoffmann, E.K., Yoder, B.K., Schwab, A., et al., 2010. Directional cell migration and chemotaxis in wound healing response to PDGF-AA are coordinated by the primary cilium in fibroblasts. Cell. Physiol. Biochem. 25, 279–292.

Schneider, C.A., Rasband, W.S., Eliceiri, K.W., 2012. NIH Image to ImageJ: 25 years of image analysis. Nat. Methods 9, 671–675.

Seeley, E.S., Nachury, M.V., 2010. The perennial organelle: assembly and disassembly of the primary cilium. J. Cell Sci. 123, 511–518.

Shao, Y.Y., Wang, L., Welter, J.F., Ballock, R.T., 2012. Primary cilia modulate Ihh signal transduction in response to hydrostatic loading of growth plate chondrocytes—1-s2.0-S8756328211012014-main.pdf. Bone 50, 79–84.

Shinozaki, S., Ohnishi, H., Hama, K., Kita, H., Yamamoto, H., Osawa, H., Sato, K., Tamada, K., Mashima, H., Sugano, K., 2008. Indian hedgehog promotes the migration of rat activated pancreatic stellate cells by increasing membrane type-1 matrix metalloproteinase on the plasma membrane. J. Cell. Physiol. 216, 38–46.

Simpson, K.J., Selfors, L.M., Bui, J., Reynolds, A., Leake, D., Khvorova, A., Brugge, J.S., 2008. Identification of genes that regulate epithelial cell migration using an siRNA screening approach. Nat. Cell Biol. 10, 1027–1038.

Skoge, M., Adler, M., Groisman, A., Levine, H., Loomis, W.F., Rappel, W.-J., 2010. Gradient sensing in defined chemotactic fields. Integr. Biol. (Camb.) 2, 659–668.

Sniedovich, M., 2006. Dijkstra's algorithm revisited: the dynamic programming connexion. Control. Cybern. 35, 599.

Stark, C., Breitkreutz, B.-J., Chatr-aryamontri, A., Boucher, L., Oughtred, R., Livstone, M.S., Nixon, J., Van Auken, K., Wang, X., Shi, X., 2011. The BioGRID interaction database: 2011 update. Nucleic Acids Res. 39, D698–D704.

Sugrue, T., Brown, J.A.L., Lowndes, N.F., Ceredig, R., 2012. Multiple facets of the DNA damage response contribute to the radioresistance of mouse mesenchymal stromal cell lines. Stem Cells 31 (1), 137–145.

Sugrue, T., Brown, J.A.L., Lowndes, N.F., Ceredig, R., 2013. Multiple facets of the DNA damage response contribute to the radioresistance of mouse mesenchymal stromal cell lines. Stem Cells 31, 137–145.

Sullivan, C., Murphy, J.M., Griffin, M.D., Porter, R.M., Evans, C.H., O'Flatharta, C., Shaw, G., Barry, F., 2012. Genetic mismatch affects the immunosuppressive properties of mesenchymal stem cells in vitro and their ability to influence the course of collagen-induced arthritis. Arthritis Res. Ther. 14, R167.

Szklarczyk, D., Franceschini, A., Kuhn, M., Simonovic, M., Roth, A., Minguez, P., Doerks, T., Stark, M., Muller, J., Bork, P., 2011. The STRING database in 2011: functional interaction networks of proteins, globally integrated and scored. Nucleic Acids Res. 39, D561–D568.

Takeda, S., Narita, K., 2012. Structure and function of vertebrate cilia, towards a new taxonomy. Differentiation 83, S4–S11.

Tarapore, P., Horn, H.F., Tokuyama, Y., Fukasawa, K., 2001. Direct regulation of the centrosome duplication cycle by the p53-p21Waf1/Cip1 pathway. Oncogene 20, 3173–3184.

Troilo, A., Alexander, I., Muehl, S., Jaramillo, D., Knobeloch, K.-P., Krek, W., 2014. HIF1α deubiquitination by USP8 is essential for ciliogenesis in normoxia. EMBO Rep. 15, 77–85.

Tummala, P., Arnsdorf, E.J., Jacobs, C.R., 2010. The role of primary cilia in mesenchymal stem cell differentiation: a pivotal switch in guiding lineage commitment. Cell. Mol. Bioeng. 3, 207–212.

van der Kraan, A.G.J., Chai, R.C.C., Singh, P.P., Lang, B.J., Xu, J., Gillespie, M.T., Price, J.T., Quinn, J.M.W., 2013. HSP90 inhibitors enhance differentiation and MITF (microphthalmia transcription factor) activity in osteoclast progenitors. Biochem. J. 451, 235–244.

van Reeuwijk, J., Arts, H.H., Roepman, R., 2011. Scrutinizing ciliopathies by unraveling ciliary interaction networks. Hum. Mol. Genet. 20, R149–R157.

Verghese, E., Zhuang, J., Saiti, D., Ricardo, S.D., Deane, J.A., 2011. In vitro investigation of renal epithelial injury suggests that primary cilium length is regulated by hypoxia-inducible mechanisms. Cell Biol. Int. 35, 909–913.

Walsby, E.J., Lazenby, M., Pepper, C.J., Knapper, S., Burnett, A.K., 2013. The HSP90 inhibitor NVP-AUY922-AG inhibits the PI3K and IKK signalling pathways and synergizes with cytarabine in acute myeloid leukaemia cells — Walsby-2013 — British Journal of Haematology — Wiley Online Library. Br. J. Haematol. 161, 57–67.

Wang, L., Benedito, R., Bixel, M.G., Zeuschner, D., Stehling, M., Sävendahl, L., Haigh, J.J., Snippert, H., Clevers, H., Breier, G., et al., 2012. Identification of a clonally expanding haematopoietic compartment in bone marrow. EMBO J. 32 (2), 219–230.

Wann, A.K., Thompson, C.L., Chapple, J.P., Knight, M.M., 2013. Interleukin-1β sequesters hypoxia inducible factor 2α to the primary cilium. Cilia 2, 17.

Weatherbee, S.D., Niswander, L.A., Anderson, K.V., 2009. A mouse model for Meckel syndrome reveals Mks1 is required for ciliogenesis and Hedgehog signaling. Hum. Mol. Genet. 18, 4565–4575.

Wicher, D., 2012. Functional and evolutionary aspects of chemoreceptors. Front. Cell. Neurosci. 6, 48.

Yan, X., Zhu, X., 2012. Branched F-actin as a negative regulator of cilia formation. Exp. Cell Res. 319, 147–151.

Yang, Y., Roine, N., Mäkelä, T.P., 2013. CCRK depletion inhibits glioblastoma cell proliferation in a cilium-dependent manner. EMBO Rep. 14, 741–747.

Yoneda, A., Multhaupt, H.A.B., Couchman, J.R., 2005. The Rho kinases I and II regulate different aspects of myosin II activity. J. Cell Biol. 170, 443–453.

Zalli, D., Bayliss, R., Fry, A.M., 2012. The Nek8 protein kinase, mutated in the human cystic kidney disease nephronophthisis, is both activated and degraded during ciliogenesis. Hum. Mol. Genet. 21, 1155–1171.

Zhu, D., Shi, S., Wang, H., Liao, K., 2009a. Growth arrest induces primary-cilium formation and sensitizes IGF-1-receptor signaling during differentiation induction of 3T3-L1 preadipocytes. J. Cell Sci. 122, 2760–2768.

Zhu, D., Shi, S., Wang, H., Liao, K., 2009b. Growth arrest induces primary-cilium formation and sensitizes IGF-1-receptor signaling during differentiation induction of 3 T3-L1 preadipocytes—Supp material. J. Cell Sci. 122, 2760–2768.